Project	**IEEE 802.16 Broadband Wireless Access Working Group** <http://ieee802.org/16>
Title	**Space-Time Power Control for MIMO Transmissions**
Date Submitted	**2008-07-07**
Sources	Kim Olszewski E-mail: kolszewski@zteusa.com ZTE USA, Inc 10105 Pacific Heights Blvd, Suite 250 San Diego, CA 92121
Re:	IEEE 802.16m-08/024 - Call for Comments and Contributions on Project 802.16m System Description Document (SDD). Topic: Power Control
Abstract	This document describes a proposal for power control within 802.16m systems.
Purpose	To review and adopt the proposed text in the next revision of the SDD.
Notice	
Release	
Patent Policy	

Space-Time Power Control for MIMO Transmissions

Kim Olszewski
ZTE USA, Inc.

1 Introduction

Multiple-input, multiple-output (MIMO) communication systems employ $N_T > 1$ transmit antennas and $N_R \geq 1$ receive antennas. An N_R-by-N_T MIMO channel may be decomposed into $N_S \leq \min(N_T, N_R)$ independent spatial subchannels when the MIMO channel matrix is a full-rank matrix. MIMO system channel conditions typically vary with time so the N_S spatial subchannels experience different subchannel conditions that results in different received signal post-processing SINRs. Consequently, the data rates that may be supported by the spatial subchannels may be different for the N_S spatial subchannels.

A key challenge in a MIMO system implementation is the specification of antenna transmit powers to use for spatial subchannel data transmissions. Transmit power control methods may reduce inter- and intra-cell interference, compensate for signal fades and path loss, and facilitate network functions such as BS selection . In addition, for OFDM-based transmissions subcarrier power concentration is allowed. A base station can specify the amount of power to be allocated to subcarriers and thereby provide for improvements in coverage, received subcarrier SINR values, and improved subcarrier frequency reuse.

Power control methods can be categorized as open- or closed-loop. Open-loop methods compensate for slow signal power variations associated with signal propagation path length and signal shadowing. However, open loop power control is more subject to calibration error, channel quality measurement errors, and fast time-varying channels. To correct for errors associated with open loop power control and to track fast time-varying channels and interference a form of closed loop power control is also required.

In closed-loop power control a receiver adaptively commands a transmitter to update its transmit power level based on received channel quality measurements (e.g. SINR) of the transmitter's signal. The control loop has to compensate for small-scale fading, hence, the feedback rate should be on the order of Doppler frequency for optimal results.

Closed-loop power control performance may be affected by power control parameters such as power control step size, power-update rate, channel quality measurement accuracy, power update feedback delay, and the reliability of power increment or decrement commands in the form of power control bits (PCBs).

Within in the literature feedback delay is found to be the most critical closed-loop power control parameter. To minimize feedback delay predictive closed-loop power control may be used. In predictive closed-loop power control, future received channel quality SINR values are predicted using previous and present SINR estimates. PCBs are subsequently generated using predicted SINR values rather than SINR estimates. Thus PCBs based on predicted SINR values better track changes in channel and interference-plus-noise power which occur during closed-loop processing.

Multiple step-size power control methods were also introduced in the literature to improve closed-loop power control performance. Power control step (PCS) sizes that better inversely match variations in received SINR will improve closed-loop power control tracking performance and increase network capacity. A larger power control step size is better suited to track rapid deviations in received SINR; slow deviations in received SINR are better tracked using a smaller step size.

However, power control-loop error increases if PCSs do not inversely match changes in received SINR. A type of error called slope-overload error results if the PCS size is too small to inversely track segments of received SINR that have fast or abruptly changing slopes. For example, slope-overload will arise if the PCS size is fixed at 1 dB, the received interference-plus-noise power is constant, and received signal power decreases at 2 dB per subframe. Conversely, if the PCS size is too large in segments of received SINR that have small slopes a type of error called granular error will arise. A solution to the slope-overload

and granular errors is the incorporation of PCS size adaptation into closed-loop power control. PCS size adaptation must optimally set power control step sizes in accordance with changes in received SINR.

A comparison of non-predictive, predictive and adaptive step-size closed-loop power control methods are given in the references. Results show that predictive closed-loop power control affords better performance in terms of network capacity when compared to both non-predictive and adaptive step-size closed loop power control. Predictive closed-loop power control showed significant improvement for low mobility MSs and performs better than non-predictive and adaptive step-size closed-lop power control under all mobility conditions. Adaptive step-size closed-loop power control gives better performance for a limited MS velocity range compared to conventional closed-loop power control.

This contribution describe a closed-loop power control technique to control the transmit power of the spatial streams in a MIMO system utilizing only post-processing SINR values and PCBs. The proposed technique recommends the usage of SINR prediction and adaptive PCS size prediction within a closed-loop power control implementation. As described below, SINR values may be adaptively predicted using previous and present SINR estimates. The predicted SINR values are subsequently used to generate PCBs. Adaptive SINR prediction may help lessen the incorrect setting of PCBs. Using the proposed technique PCS sizes for a transmitter may be adaptively predicted using previous and present detected PCBs. Slope-overload and granular error arises due to non-optimal PCS sizes. Adaptive PCS sizes help lessen slope-overload and granular errors. Another advantage in using received PCBs for adaptively predicting PCSs is that no only 1-bit power command signals are required for multiple step-size power control. In contrast, if multiple size PCSs (2 or more bits in length) were transmitted extra bandwidth would be required.

2 Signal Model for Power Control

To describe the signals for the proposed power control technique we will use a downlink signal model. The uplink signal model will be similar. The following notation is used in the description:

- N_T denotes the number of BS transmit antennas.
- N_R denotes the number of MS receive antennas.
- $N_S \leq \min(N_T, N_R)$ denotes the number of independent spatial streams transmitted by the BS.
- $\mathbf{W} \in \mathbb{C}^{N_T \times N_S}$ denotes the linear precoding matrix for the BS.
- $\mathbf{P} \in \mathbb{R}^{N_T \times N_S}$ denotes the diagonal stream power loading matrix for the BS with diagonal elements $P_{Tx,i}$, $i = 1, 2, \ldots, N_S$.
- $\mathbf{s} \in \mathbb{C}^{N_S \times 1}$ denotes the data symbol vector transmitted by the BS.
- $\mathbf{H} \in \mathbb{C}^{N_R \times N_T}$ denotes the MS's channel matrix. The (i, j)th element of $\mathbf{H}$ represents the channel gain and phase associated with the signal path from MS transmit antenna j to BS receive antenna i. The channel matrices are assumed fixed during the transmission duration but may change independently from one subframe to the next.

The downlink signal transmitted by the BS may be written as

$$\mathbf{x} = \mathbf{WPs} \in \mathbb{C}^{N_T \times 1} \tag{1}$$

We assume that the data symbol vector $\mathbf{s}$ has normalized unit energy and the following mean and covariance

$$E[\mathbf{s}] = \mathbf{0} \tag{2}$$

$$\mathbf{R_s} = E[\mathbf{ss}^H] = \mathbf{I}_{N_T} \tag{3}$$

where $\mathbf{I}_{N_T} \in \mathbb{R}^{N_T \times N_T}$ denotes an identity matrix. The total average transmit power distributed over N_T antennas is

$$P_T = \mathrm{Tr}\left\{\mathbf{W}\mathbf{P}\mathbf{P}^H\mathbf{W}^H\right\} \tag{4}$$

where Tr denotes the trace of the matrix.

We assume that the cyclic prefix is greater in length than the channel delay spread and that the maximum Doppler frequency is much smaller than the OFDM symbol subcarrier spacing. We can therefore ignore any inter-subcarrier interference caused by Doppler frequency spreading. Under these assumptions the received MS signal may be written as

$$\mathbf{y} = \mathbf{H}\mathbf{x} + \mathbf{n} \in \mathbb{C}^{N_R \times 1} \tag{5}$$

where $\mathbf{n} \in \mathbb{C}^{N_R \times 1}$ denotes an interference-plus-noise vector with the following mean and covariance

$$E[\mathbf{n}] = \mathbf{0} \tag{6}$$

$$\mathbf{R}_{\mathbf{n}} = E[\mathbf{n}\mathbf{n}^H] \in \mathbb{C}^{N_R \times N_R} \tag{7}$$

To see the impact of power changes on the received signal we set $N_S = 2$, $N_T = 2$, and $N_R = 2$. The above received signal can then be written as

$$\begin{bmatrix} y_1 \\ y_2 \end{bmatrix} = \begin{bmatrix} h_{11} & h_{12} \\ h_{21} & h_{22} \end{bmatrix} \begin{bmatrix} w_{11} & w_{12} \\ w_{21} & w_{22} \end{bmatrix} \begin{bmatrix} P_{Tx,1} & 0 \\ 0 & P_{Tx,2} \end{bmatrix} \begin{bmatrix} s_1 \\ s_2 \end{bmatrix} + \begin{bmatrix} n_1 \\ n_2 \end{bmatrix} \tag{8}$$

$$= \begin{bmatrix} h_{11}\left(w_{11}P_{Tx,1}s_1 + w_{12}P_{Tx,2}s_2\right) + h_{12}\left(w_{21}P_{Tx,1}s_1 + w_{22}P_{Tx,2}s_2\right) \\ h_{21}\left(w_{11}P_{Tx,1}s_1 + w_{12}P_{Tx,2}s_2\right) + h_{22}\left(w_{21}P_{Tx,1}s_1 + w_{22}P_{Tx,2}s_2\right) \end{bmatrix} + \begin{bmatrix} n_1 \\ n_2 \end{bmatrix} \tag{9}$$

where $P_T = P_{Tx,1} + P_{Tx,2}$. It is easily seen that an increase/decrease in $P_{Tx,1}$ or $P_{Tx,2}$ will be observed in both MS receive antennas. This coupling complicates the space-time power control process.

The post-processing SINRs of the spatial streams are dependent on the particular MIMO receive signal processing implemented at the MS. Post-processing SINRs may be independent or coupled via "crosstalk" among the spatial streams. For a zero-forcing (ZF) receiver the detected spatial streams are decoupled by the receiver signal processing so changing the transmit power of one spatial stream does not affect the post-processing SINRs of the other spatial streams. In contrast, for the MMSE or Wiener filter MIMO receiver, the post-processing SINR of each spatial stream is coupled to the other spatial streams. Hence for this case an increase or decrease in transmit power of one spatial stream will affect the post-processing SINRs of the other spatial streams.

More specifically, it is shown in [2,3,4] that the post-processing SINRs of the ith spatial stream for a zero-forcing receiver and a Wiener filter receiver may be written as

$$SINR_i^{\mathrm{ZF}} = \frac{1}{\sigma_{\mathbf{n}}^2\left[\left(\mathbf{H}^H\mathbf{H}\right)^{-1}\right]_{ii}} \tag{10}$$

and

$$SINR_i^{\mathrm{WF}} = \mathbf{b}_i^H\mathbf{H}^H\mathbf{R}_{\mathbf{n}_i}^{-1}\mathbf{H}\mathbf{b}_i \tag{11}$$

where $\left[\left(\mathbf{H}^H\mathbf{H}\right)^{-1}\right]_{ii}$ denotes the ith diagonal element of $\left(\mathbf{H}^H\mathbf{H}\right)^{-1}$, $\mathbf{b}_i$ denotes the ith column of the matrix product $\mathbf{B}_k = \mathbf{W}\mathbf{P}$, and

$$\mathbf{R}_{\mathbf{n}_i} = E\left[\mathbf{n}_i\mathbf{n}_i^H\right] = \mathbf{R}_{\mathbf{n}} + \mathbf{H}\left(\mathbf{B}_k\mathbf{B}_k^H - \mathbf{b}_i\mathbf{b}_i^H\right)\mathbf{H}^H \in \mathbb{C}^{N_R \times N_R} \tag{12}$$

the covariance matrix of $\mathbf{n}_i$ which denotes the interference-plus-noise associated with the ith spatial stream. From the above equations we see that the $SINR_i^{\mathrm{ZF}}$ values are independent. In contrast, we see that the $SINR_{k,i}^{\mathrm{WF}}$ values are correlated or coupled due to matrix $\mathbf{B}_k$ within the equation for $\mathbf{R}_{\mathbf{n}_i}$.

Our proposed approach to simplify and decouple the space-time power control technique is to uniformly distribute power over all transmit antennas and to equally allocate power increments/decrements to all transmit antennas. Let P_T/N_T denote the average per-antenna power. We can then write

$$\mathbf{b}_i = (P_T/N_T)\,\mathbf{w}_i \tag{13}$$

$$\mathbf{B}_k\mathbf{B}_k^H = (P_T/N_T)^2\,\mathbf{W}\mathbf{W}^H \tag{14}$$

and

$$\mathbf{R}_{\mathbf{n}_i} = \mathbf{R}_{\mathbf{n}} + (P_T/N_T)^2\,\mathbf{H}\left(\mathbf{W}\mathbf{W}^H - \mathbf{w}_i\mathbf{w}_i^H\right)\mathbf{H}^H \tag{15}$$

The total average transmit power P_T for all N_T transmit antennas may be allocated to the data streams using P_T/N_T so the total transmit power is uniformly distributed. This is true even if only some subset of the antennas is used for data transmission. In this case $N_S < N_T$ so the total power used is less than P_T and equal to $N_T \cdot P_T/N_T$.

3 Description of the Proposed Closed-loop Power Control Technique

Figures 1 and 2 show BS and MS block diagrams for the proposed closed-loop power control technique. Figures 1 and 2 will be used as a references to describe the proposed technique. The proposed power control technique is described in the subsections below using only MS operations. The BS functions in a similar manner so a description of its operation is not needed.

Before proceeding with the description and more detail we briefly overview the approach beginning with the BS. The BS first specifies a power increment or decrement for an MS's uplink transmissions using a single power control bit (PCB). Each BS-specified power control bit indicates a power increment or decrement for an MS's transmitter. A power control bit equal to a logical 0 commands an MS power increase; a power control bit equal to a logical 1 commands an MS power decrease. The BS periodically transmits PCBs to an MS in a downlink subframe control field. The control field may support a single PCB or multiply copies of the PCB if repetition coding is used for increased reliability. Hence the rate at which MS power control adjustments can occur is based on the transmit rate of the downlink control field. At the receive side a recipient MS detects the BS-transmitted PCB. The detected PCB is then used to derive a Power Control Step (PCS) for the MS's transmitter. The MS adjusts its transmitter's power amplifier in accordance with the derived PCC. We now proceed and describe some details of the proposed technique.

3.1 SINR Generator

Typical signal quality estimates used for closed-loop power control are received signal power estimates or estimates of the ratio of received signal power to interference-plus-noise power (SINR). Results within the references show that SINR-based power control methods have better performance than signal power estimates only. An important advantage of an SINR-based power control method is that average transmit power can be reduced as network load decreases, thereby reducing network interference and conserving power.

A problem that may arise when using SINR-based closed-loop power control is that a positive feedback situation may arise. To clarify the problem consider a number of MSs communicating within the boundaries of cell edges. Suppose one of the MSs detects a BS-transmitted PCB that specifies a power increase in

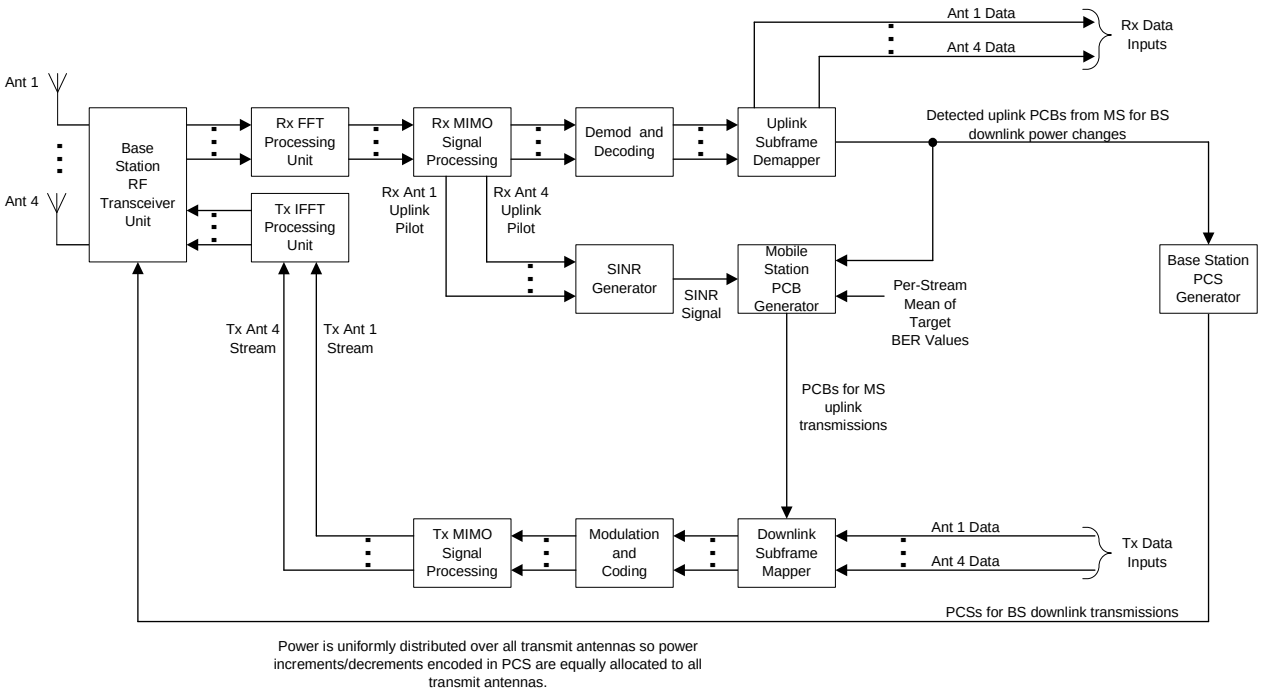

Figure 1: BS functional blocks for closed-loop power control.

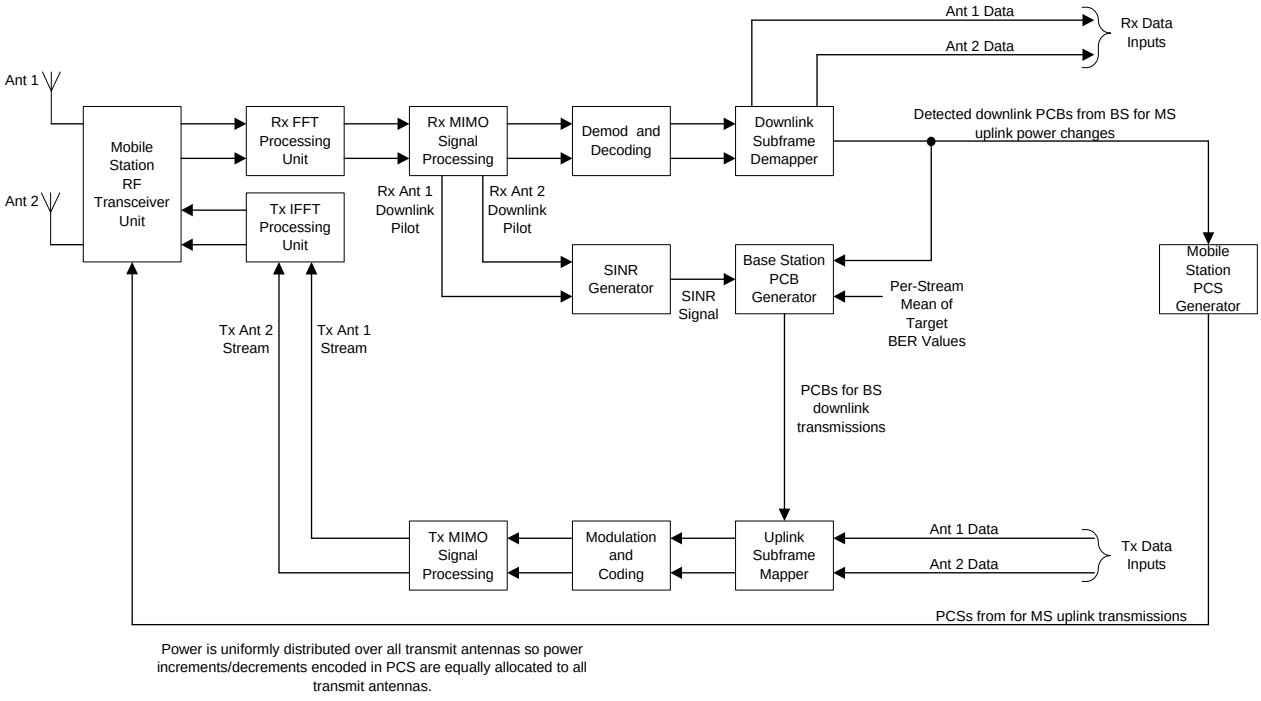

Figure 2: MS functional blocks for closed-loop power control. The block diagram only shows two antennas for simplicity. However, the maximum number of antennas is four.

order to meet a required QoS level. Based on the detected PCB the MS increases it transmit power which may result in increased interference to the other nearby MSs in the network. Hence, in response the other MSs increase their transmit power which further increases network interference. The process continues until all MSs are at their maximum allowed transmit power. If better estimates of SINR are obtained this problem is lessened.

More accurate SINR values may be computed using a pilot signal as a reference rather than a detected data signal. This is due to the fact that a pilot signal has a constant or slowly varying power level in contrast to a data signal that typically varies more in power in order to accommodate data rate changes. Data signals are also more difficult to track for power control purposes.

In a MIMO system with N_T transmit and N_R receive antennas the number of independent and resolvable spatial streams is $N_S \leq \min(N_T, N_R)$ if the MIMO channel matrix is of full-rank. Each spatial stream is associated with a post-processing SINR which is the measured after MIMO receiver signal processing.

The example mobile station SINR Generator of Figure 2 uses two dedicated downlink pilots as reference signals for post-processing SINR predictions. Given received versions of the reference pilots as inputs the SINR Generator first computes estimates of the post-processing SINR for each spatial stream. Given these SINR estimates the SINR Generator then combines the SINR estimates into a single estimate by computing their average (other statistics may also be used). The SINR Generator then computes a predicted SINR value $\widehat{SINR}_{BS}[n]$ using the single SINR estimate just computed and past SINR estimates computed in the same manner. For example, a simple least mean square (LMS) or Kalman algorithm may used for the SINR predictor to output $\widehat{SINR}_{BS}[n]$. Note that SINR prediction step is optional but performance comparisons in the references have shown that predictive power control typically performs better.

3.2 Base Station Power Control Bit Generator

The post-processing SINR Predictor values $\widehat{SINR}_{BS}[n]$ are then input to the Base Station PCB Generator. The Base Station PCB Generator outputs a binary signal comprised of power control bit samples $PCB_{BS}[n]$. The PCBs samples specify power increments or decrements for BS-to-MS downlink transmissions. The PCB samples will be transmitted to the BS; the PCB samples will then be used by the BS to adjust its power for downlink transmissions to the MS.

To generate PCB samples the Base Station PCB Generator compares samples $\widehat{SINR}_{BS}[n]$ output from the SINR Generator with target SINR samples $SINR_{BS}[n]$. A target SINR sample $SINR_{BS}[n]$ is the post-processing SINR needed to achieve the target BER for a particular data rate or QoS.

To generate a target SINR sample $SINR_{BS}[n]$ the Base Station PCB Generator first generates a bit error rate (BER) signal with samples $\widehat{BER}_{BS}[n]$. For example, an estimate of the BER as a function of $\widehat{SINR}_{BS}[n]$ and an M-QAM modulation parameter M is as follows:

$$\widehat{BER}_{BS}[n] = \frac{4}{\log_2 M}\left(1 - \frac{1}{\sqrt{M}}\right) Q\left(\sqrt{\frac{3}{M-1}\widehat{SINR}_{BS}[n]}\right) \tag{16}$$

Samples $\widehat{BER}_{BS}[n]$ of the estimated bit error rate signal produced by the Base Station PCB Generator are then used to generate a downlink SINR setpoint sample $SINR_{BS}[n]$. A target or reference BER value from a set of target BER values BER^1_{BS}, $i = 1, 2, \ldots, P$, is also used for this purpose. Note that the target BER values may be per-stream mean BERs if a multi-codeword or horizontal MIMO technique is the mode of operation being used. Given a sample $\widehat{BER}_{BS}[n]$ and a target BER value BER^i_{BS} the Base Station PCB Generator outputs an SINR setpoint sample $SINR_{BS}[n]$ using a map such as the following

$$SINR_{BS}[n] = \begin{cases} SINR^{SP}_{Up} & \text{if } BER^i_{BS} \leq \widehat{BER}_{BS}[n] \\ SINR^{SP}_{Down} & \text{if } \widehat{BER}_{BS}[n] < BER^i_{BS} \end{cases} \tag{17}$$

Samples $SINR_{BS}[n]$ are SINR values required to meet a specified target BER. Samples BER^i_{BS}, $i = 1, 2, \ldots, P$, of the QoS Reference Signal may be bit error rate values set in accordance with a downlink quality of service. For example, if $\widehat{BER}_{BS}[n]$ is too high for a specified downlink channel QoS indexed by BER^i_{BS} then $SINR_{BS}[n]$ would be set to $SINR^{SP}_{Up}$ specifying that a higher SINR is required . Alternatively, if $\widehat{BER}_{BS}[n]$ is less than the target BER BER^i_{BS} the setpoint sample $SINR_{BS}[n]$ would be set to $SINR^{SP}_{Down}$ specifying that a lower SINR is required. The chosen value $SINR^{SP}_{Down}$ may be a decrement so that the power is minimized and interference is decreased.

Given input samples $\widehat{SINR}_{BS}[n]$ and $SINR_{BS}[n]$ the Base Station PCB Generator then outputs a base station PCB sample $PCB_{BS}[n]$ using the map

$$PCB_{BS}[n] = \begin{cases} 1 \text{ (BS power decrease)} & \text{if } SINR_{BS}[n] < \widehat{SINR}_{BS}[n] \\ 0 \text{ (BS power increase)} & \text{if } SINR_{BS}[n] \geq \widehat{SINR}_{BS}[n] \end{cases} \tag{18}$$

Samples $PCB_{BS}[n]$ form a BS power control signal that is used by the BS to adjust its downlink power when communicating with the MS. If $PCB_{BS}[n] = 0$ a BS power increase is specified by the MS; if $PCB_{BS}[n] = 1$ a BS power decrease is specified by the MS. The resulting PCB sample $PCB_{BS}[n]$ is mapped onto the the MS's uplink subframe and subsequently transmitted back to the BS where it is detected.

3.3 Mobile Station Power Control Step Size Generator

At the base station PCB samples for the MS are computed using the map

$$PCB_{MS}[n] = \begin{cases} 1 \text{ (MS power decrease)} & \text{if } SINR_{MS}[n] < \widehat{SINR}_{MS}[n] \\ 0 \text{ (MS power increase)} & \text{if } SINR_{MS}[n] \geq \widehat{SINR}_{MS}[n] \end{cases} \tag{19}$$

where $SINR_{MS}[n]$ and $\widehat{SINR}_{MS}[n]$ denote SINR setpoint and predicted mobile station received SINR values. At the BS values $PCB_{MS}[n]$, $SINR_{MS}[n]$ and $\widehat{SINR}_{MS}[n]$ are generated using the same processing as described above for the MS. See Figure 1 for clarification.

Waveform quantization is a signal compression technique in which samples of a signal are mapped to discrete steps or levels; each step is represented by a minimal number of bits for compression purposes. Differential or predictive quantization is a waveform quantization method in which the difference between a sample and a predicted sample is quantized rather than the sample. Several adaptive step-size methods for differential quantization have been described in the references. Continuously Variable Slope Delta-Modulation (CVSD) is a well-proven and well-established differential waveform quantization method with adaptive step-size adjustment. By adapting the step-size to changes in slope of a differenced signal, CVSD is better able to quantize differenced signals. When the slope of a signal changes too quickly for CVSD to track, step-size is increased. Conversely, when the slope changers too slowly, step-size is decreased. In this manner slope overload and granular errors may be reduced.

At the MS power control bit samples $PCB_{MS}[n]$ are detected from BS-to-MS downlink transmissions. Given detected power control bits samples $PCB_{BS}[n]$ the MS's Power Control Step Size Generator implements PCS size adaptation using a CVSD circuit such as that shown in Figure 4. As shown in Figure 4 the CVSD circuit is comprised of a slope-overload detector and an integrator. The adaptation mechanism implemented by the Power Control Step Size Generator is based on PCB patterns detected during segments of slope-overload. From the map above for samples $PCB_{MS}[n]$ it is clear that in the absence of channel errors, segments of slope-overload error will be manifested by runs of consecutive $PCB_{MS}[n]$ values of logic zero or one. For example, a PCB run pattern associated with slope overload may be bit sequence of 0,0,0,0 or 1,1,1,1. These patterns are used by the Power Control Step Size Generator for PCS size adaptation. Referring to Figure 4 the process is summarized in the following paragraphs of this section.

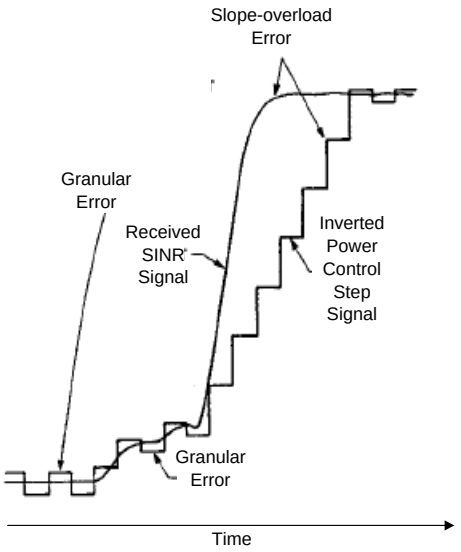

Figure 3: Illustration of slope overload and granular errors. Inverted PCS signal should ideally match received SINR signal. Slope-overload error results if the PCS size is too small to inversely track segments of received SINR that have fast or abruptly changing slopes. If the PCS size is too large in segments of received SINR that have small or zero slopes a type of error called granular error will arise.

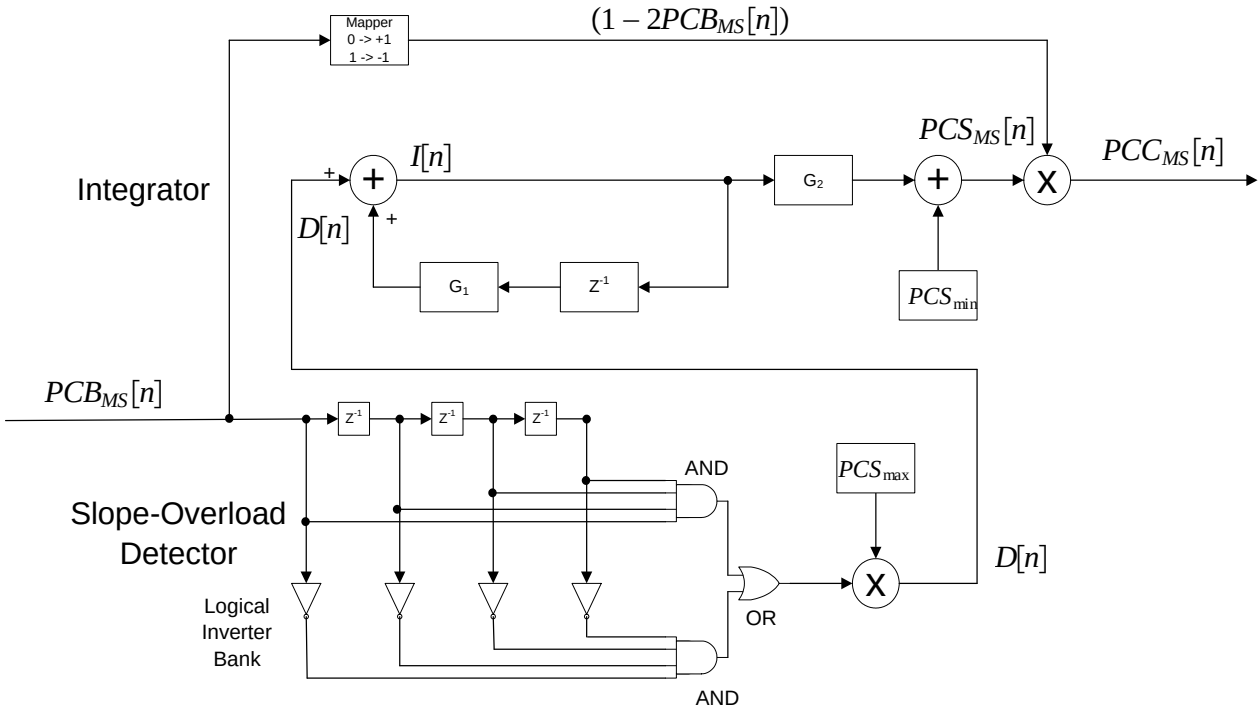

Figure 4: Example Power Control Step Size generator comprised of a slope-overload detector and an integrator.

The Slope-overload Detector of the Power Control Step Size Generator first computes

$$D[n] = \begin{cases} PCS_{\max} & \text{if } \{PCB_{MS}[j],\ j = n-3, ..., n\} = \{0,0,0,0\} \\ PCS_{\max} & \text{if } \{PCB_{MS}[j],\ j = n-3, ..., n\} = \{1,1,1,1\} \\ 0 & \text{otherwise} \end{cases} \tag{20}$$

where positive real-values $PCS_{\max}$ is the maximum allowed power control step size allowed.

Given $D[n]$ the Integrator of the Power Control Step Size Generator then computes

$$I[n] = G_1 I[m-1] + D[n] \tag{21}$$

followed by the MS's power control step sample

$$PCS_{MS}[n] = G_2 I[n] + PCS_{\min} \tag{22}$$

where positive real-value $PCS_{\min}$ is the minimum allowed power control step size allowed. Samples $PCS_{MS}[n]$ are constrained to lie within the interval [$PCS_{\min}$,$PCS_{\max}$]. Appropriate values for parameters G_1, G_2, $PCS_{\min}$ and $PCS_{\max}$ can be determined by determined by computer simulations or set in accordance with the standard. For example, $PCS_{\min}$ and $PCS_{\max}$ values of 0 and 2.0 may be used.

It should be emphasized that $PCS_{MS}[n]$ is computed using a set of received PCB samples to adjust the MS's transmitter power rather than a single PCB value. Thus the Power Control Step Size Generator incorporates the memory or autocorrelation statistic of the received PCB time series $\{PCB_{MS}[j],\ j = n-3, ..., n\}$ into its operation. This approach provides better power control step sizes for the MS's transmitter and thereby allows better channel tracking for the power control loop. Also, the set of received PCB samples used can be changed in length. For example, an alternative set is $\{PCB_{MS}[j],\ j = n-5, ..., n\}$ with six $PCB_{MS}[n]$ values.

Given the received $PCB_{MS}[n]$ bit from the BS and the power control step $PCS_{MS}[n]$ the Power Control Step Size Generator next updates the MS's power control step sample as

$$PCS_{MS}[n] = (1 - 2PCB_{MS}[n])PCS_{MS}[n] \tag{23}$$

Note that $PCC_{MS}[n]$ is computed by multiplying $PCS_{MS}[n]$ with a detected binary-to-bipolar mapped value $(1 - 2PCB_{MS}[n])$. Recall that if $PCB_{MS}[n] = 0$ a MS power increase is specified by the BS and if $PCB_{MS}[n] = 1$ a MS power decrease is specified by the BS. Hence, the update specifies the direction of the power control step $PCS_{MS}[n]$.

Note that the power control step $PCS_{MS}[n]$ is increased to reduce slope-overload errors and decreased to reduce granular errors. Also, PCS increments and decrements for the MS's transmitter are not assigned by the BS via downlink signaling. The MS can generate optimal PCSs in an autonomous manner thereby reducing signaling overhead and associated delays which would occur if the BS transmitted PCS values for the MS to use.

Figures 5 and 6 show example plots output by the Power Control Step Size Generator. The parameters used are as follows: $PCS_{\max} = 2$, $PCS_{\min} = 0$, $G_1 = 0.35$, and $G_2 = 0.15$. For comparison the first three plots show the results for a fixed PCS of 1 dB. The second group of three plots shows the improvement using the Power Control Step Size Generator described above.

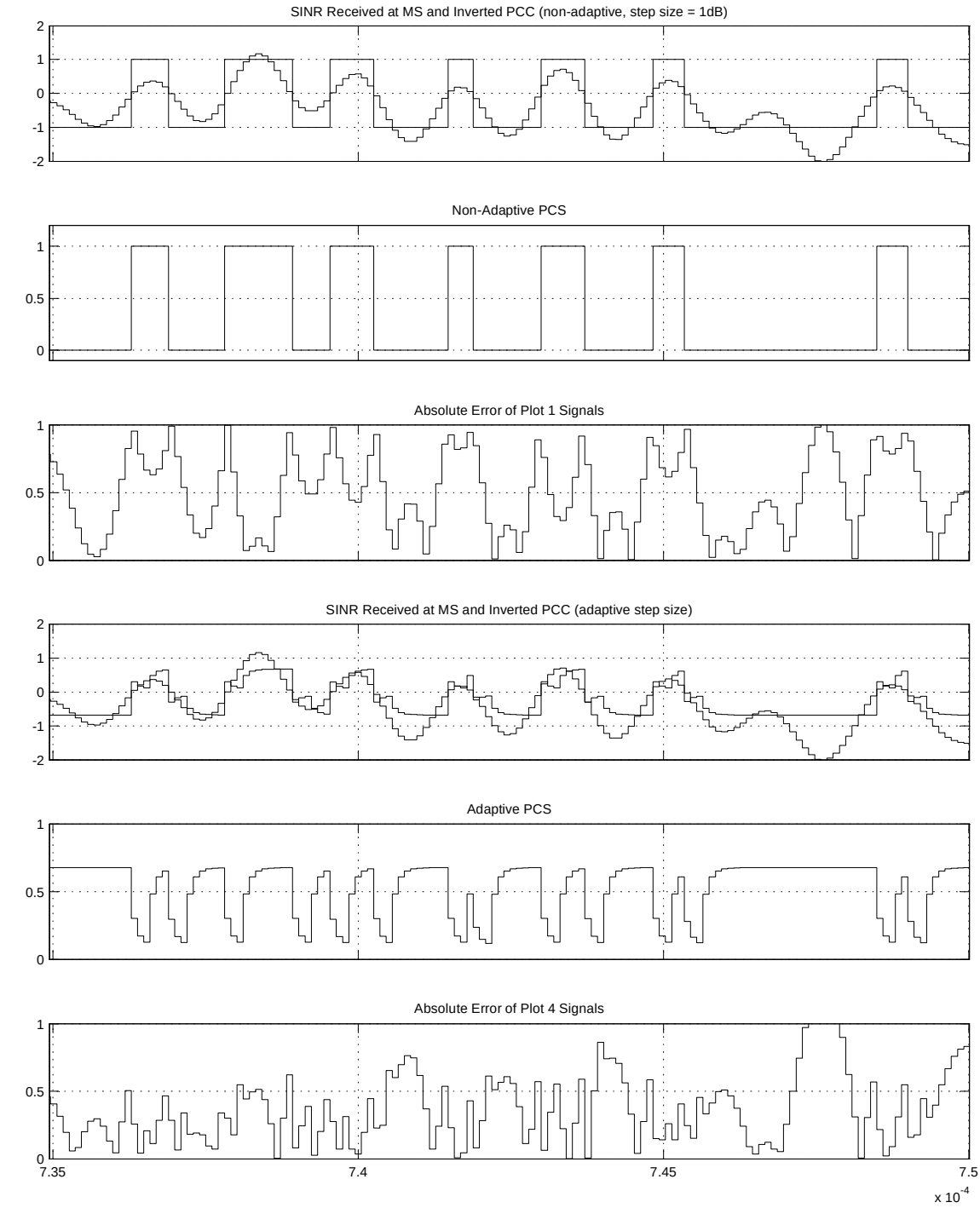

Figure 5: Example of signals from Power Control Step Size Generator.

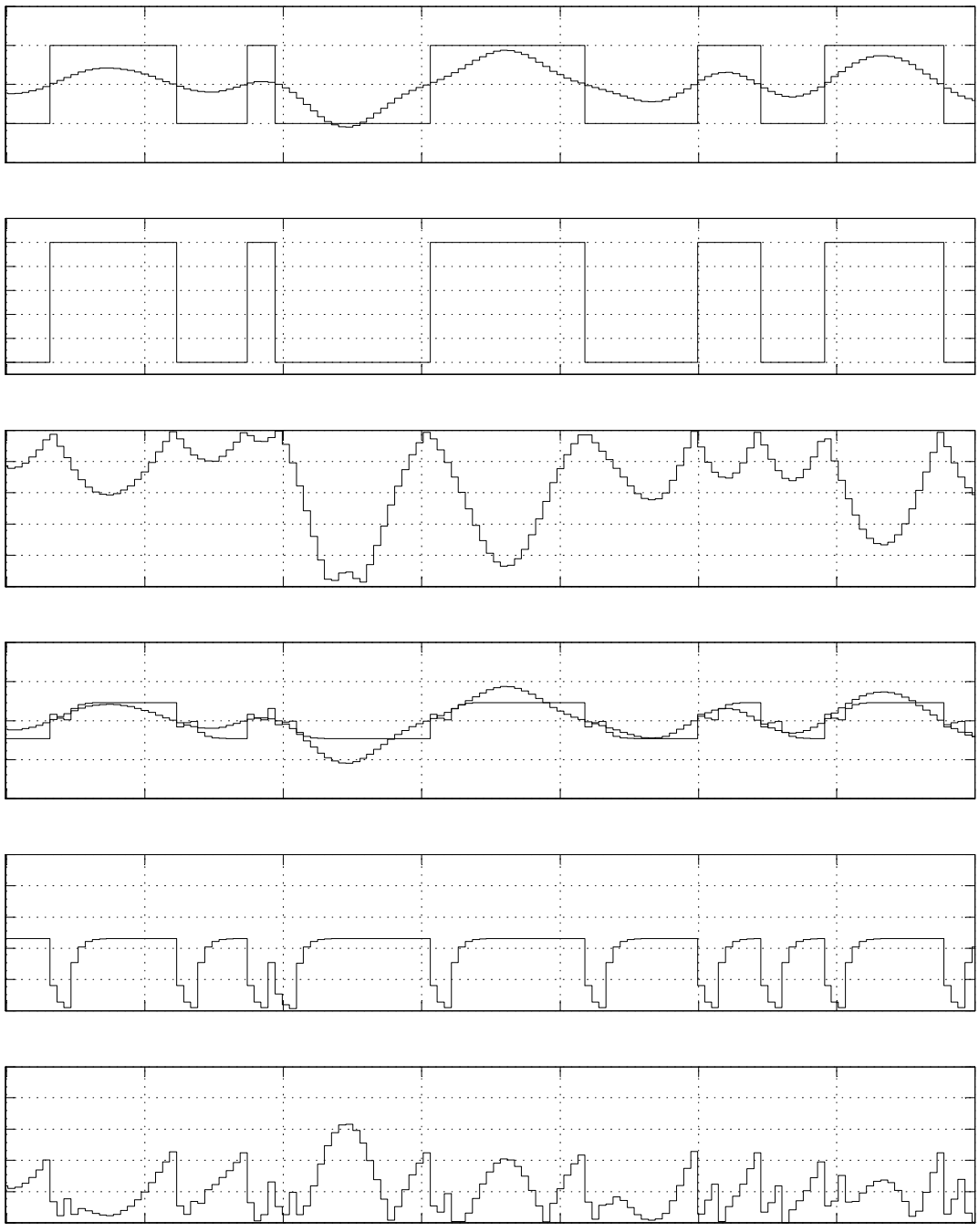

Figure 6: Example of signals from Power Control Step Size Generator.

4 References

1. Lim Sim, M. et al, “Performance Study of Closed-loop Power Control Algortihms for a Cellular CDMA System,” Vol. 48, No.3, pp. 911-921, IEEE Trans. on Vehicular Technology., May 1999.

2. Daniel P. Palomar, “Unified Design of Linear Transceivers for MIMO Channels,” in the book Smart Antennas – State-of-the-Art, Chapter 3, EURASIP Hindawi Book Series, T. Kaiser and A. Bourdoux, Editors, 2005.

3. Daniel P. Palomar, John M. Cioffi, and Miguel A. Lagunas, “Joint Tx-Rx Beamforming Design for Multicarrier MIMO Channels: A Unified Framework for Convex Optimization,” IEEE Trans. Signal Proc., Vol. 51, No. 9, Sept. 2003.

4. D. P. Palomar, “A unified framework for communications through MIMO channels,” Ph.D. dissertation, Technical University of Catalonia (UPC), Barcelona, Spain, May 2003.

5. Mizuguchi, H.et al, "Performance Evaluation on Power Control and Diversity of Next-Generation CDMA Systems," IEICE Trans.Commun., Vol. E81-B No.7, pp.1345-1354, July 1998.

6. Shunsuke, S. et al, “SIR-Based Transmit Power Control of Reverse Link for Coherent DS-CDMA Mobile Radio," IEICE Trans.Commun., Vol. E81-B No.7, pp.1508-1516, July 1998.

7. Wen, J.et al, "Performance of Short-term Fading Prediction-based Power Control Method for DS-CDMA Mobile Radio," IEICE Trans. Commun., Vol. E81-B No.6, pp.1231-1237, June 1998.

8. Lyu, D. et al, "Capacity Evaluation of a Forward Link DS-CDMA Cellular System with Fast TPC Based on SIR," IEICE Trans. Commun., Vol. E83-B No.6, pp.68-76, January 2000.

9. Kikuchi, F.et al,"Effect of Fast Transmit Power Control on Forward Link Capacity of DS-CDMA Cellular Mobile Radio," IEICE Trans. Commun., Vol. E83-B No.1, pp.47-55, January 2000.

10. Kenichi Higuchi, Hidehiro Andoh, Koichi Okawa, Mamoru Sawahashi and Fumiyuki Adachi, "Experimental Evaluation of Combined Effect of Coherent Rake Combining and SIR-Based Fast Transmit Power Control for Reverse Link of DS-CMDA Mobile Radio,” IEEE J.Select. Areas of Commun, Vol.18, No.8, pp.1526-1534, August 2000.

11. Yang, Y. and Chang, "A Strength-and-SIR-Combined Adaptive Power Control for CDMA mobile Radio Channels," Vol.48 No.6 pp.1996-2004, IEEE Trans. on Vehicular Tech., November 1999.

12. Deller, J., Proakis, J., and Hansen, H., Discrete-Time Processing of Speech Signals, Macmillan Publishing Company, 1993.

13. Chockalingam, A. et al, "Performance of Closed-Loop Power Control in DS-CDMA Cellular Systems," Vol.47 No.3 pp.774-789, IEEE Trans, on Vehicular Tech., August 1998.

14. Gunnarsson, F. et all, "Dynamical Effects of Time Delays and Time Delay Compensation in Power Controlled DS-CDMA,", IEEE J. Select. Areas of Commun., Vol. 19, No.11, pp. 141-151, January 2001.

15. Jayant, N. and Noll, P. Digital Coding of Waveforms: Principles and Applications to Speech and Video, Prentice-Hall, Englewood Cliffs, NJ, 1984.

5 Proposed Text for the SDD

Closed-Loop Space-time Power Control

Multiple-input, multiple-output (MIMO) communication systems employ $N_T > 1$ transmit antennas and $N_R \geq 1$ receive antennas. An N_R-by-N_T MIMO channel may be decomposed into $N_S \leq \min(N_T, N_R)$ independent spatial subchannels when the MIMO channel matrix is a full-rank matrix. MIMO system channel conditions typically vary with time so the N_S spatial subchannels experience different subchannel conditions that results in different received signal post-processing SINRs. Consequently, the data rates that may be supported by the spatial subchannels may be different for the N_S spatial subchannels.

Open and closed-loop space-time power control will be used to control the transmit power of MIMO spatial streams. Closed-loop power control will be implemented using only received post-processing SINR values and power control bits (PCBs).that specify power increments or decrements. Adaptive SINR prediction and adaptive power control step (PCS) size prediction may be used within a closed-loop power control implementation to improve power control performance.